Biomaterials Advances 156 (2024) 213712

Contents lists available at ScienceDirect

Biomaterials Advances

journal homepage: www.journals.elsevier.com/materials-science-and-engineering-c

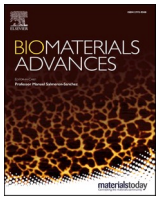

COX-2 inhibitor delivery system aiming intestinal inflammatory disorders

Ana Oliveira [a,b,c], Luísa C. Rodrigues [a,c], Diana Soares da Costa [a,c], Emanuel M. Fernandes [a,c], Rui L. Reis [a,c], Nuno M. Neves [a,c], Pedro Leão [b,c], Albino Martins [a,c,*]

[a] 3B's Research Group, I3Bs – Research Institute on Biomaterials, Biodegradables & Biomimetics of University of Minho, Headquarters of the European Institute of Excellence on Tissue Engineering & Regenerative Medicine, AvePark - Parque de Ciência e Tecnologia, Zona Industrial da Gandra, 4805-017 Barco, Guimaraes, Portugal
[b] Life and Health Sciences Research Institute (ICVS), School of Medicine, University of Minho, 4710-057 Braga, Portugal
[c] ICVS/3B's - PT Government Associate Laboratory, Braga, Guimarães, Portugal

ARTICLE INFO

Keywords:
Etoricoxib
Electrospun fibrous meshes
Colorectal
Inflammation

ABSTRACT

Selective COX-2 inhibitors such as etoricoxib (ETX) are potentially indicated for the treatment of intestinal inflammatory disorders. However, their systemic administration provokes some off-site secondary effects, decreasing the desirable local effectiveness. To circumvent such limitations, herein an ETX delivery system based on electrospun fibrous meshes (eFMs) was proposed. ETX at different concentrations (1, 2, and 3 mg mL^{-1}) was loaded into eFMs, which not affect the morphology and the mechanical properties of this drug delivery system (DDS). The ETX showed a burst release within the first 12 h, followed by a faster release until 36 h, gradually decreasing over time. Importantly, the ETX studied concentrations were not toxic to human colonic cells (i.e. epithelial and fibroblast). Moreover, the DDS loading the highest concentration of ETX, when tested with stimulated human macrophages, promoted a reduction of PGE_2, IL-8 and TNF-α secretion. Therefore, the proposed DDS may constitute a safe and efficient treatment of colorectal diseases promoted by inflammatory disorders associated with COX-2.

1. Introduction

Intestinal diseases (e.g. inflammatory bowel diseases - IBD) promoted by inflammatory disorders are of major concern among the medical community. This inflammation promotes the progression of such diseases into more serious conditions [1], with devastating consequences for patients' quality of life. IBD, such as ulcerative colitis and Crohn's disease, have a well-established association with inflammation and have also been reported to be a risk factor for the appearance of polyps and the development of colorectal cancer [1]. The involvement of the intestinal region can be at such an advanced stage that it requires surgical resection to remove the compromised tissue, followed by an intestinal anastomosis, where an uncontrolled inflammatory process could lead to anastomotic failure [2,3]. Therefore, it becomes increasingly imperative to find strategies able to control inflammation and avoid its pathogenicity in the colorectal environment.

The inflammatory processes are mediated by a key enzyme, the cyclooxygenase (COX). COX is responsible for converting arachidonic acid into prostaglandins (PGs) being present in two isoforms, COX-1 and COX-2. COX-1 is expressed constitutively in most tissues maintaining tissue homeostasis and platelet function, whereas COX-2 is characterized by its immediate early response being upregulated by inflammatory cytokines. Specifically, COX-2 catalyzes the production of PGs associated with pathological situations such as inflammation, pain, and fever [4–7]. For that reason, COX-2 is commonly overexpressed in several premalignant and malignant conditions [7], as well as in IBD conditions [8].

Selective COX-2 inhibitors or Coxibs are a class of drugs indicated to overcome selectively the pathological COX-2 action while maintaining the COX-1 activity. They potentially avoid the problems of gastric ulceration and bleeding disorders related to the use of non-selective non-steroidal anti-inflammatory drugs (NSAIDs) that act on both COX isoforms [6]. Moreover, the treatment with some selective COX-2 inhibitors has been associated with the suppression of polyps formation and the prevention of colorectal cancer [7], in addition to being associated with a lower risk of IBD worsening [9]. From the range of existing Coxibs (i.e.

* Corresponding author at: 3B's Research Group, I3Bs – Research Institute on Biomaterials, Biodegradables & Biomimetics of University of Minho, Headquarters of the European Institute of Excellence on Tissue Engineering & Regenerative Medicine, AvePark - Parque de Ciência e Tecnologia, Zona Industrial da Gandra, 4805-017 Barco, Guimaraes, Portugal.
E-mail address: amartins@i3bs.uminho.pt (A. Martins).

https://doi.org/10.1016/j.bioadv.2023.213712
Received 1 February 2023; Received in revised form 10 November 2023; Accepted 26 November 2023
Available online 29 November 2023

celecoxib, etoricoxib, rofecoxib, valdecoxib, lumiracoxib), some were withdrawn from the market due to the high risk of secondary events, leaving only celecoxib and etoricoxib (ETX) for medical use [9]. ETX (5-Chloro-6′-methyl-3-[4-(methylsulfonyl) phenyl]-2,3′-bipyridine) is a second generation of COX-2 inhibitors, used for analgesic and anti-inflammatory purposes. However, its oral or systemic administration is still associated with cardiovascular toxicity [10–12]. Therefore, it is increasingly urgent to find strategies to overcome these off-site effects.

Colon drug delivery systems (DDS) are an interesting strategy to reduce undesirable side effects. They are characterized by the ability to release drugs in the colonic environment, avoiding their degradation by the gastric pH [13]. Among the DDS, electrospun fibrous meshes (eFMs) are polymeric substrates with the potential to be loaded with different drugs and to be locally implanted. DDS based on eFMs [14–18] also offer the possibility to control the drugs' release profile and to improve the bioavailability of poorly water-soluble drugs. These substrates, in addition to the high specific surface area, exhibit high porosity [19] enabling the diffusion of the released drugs, as well as the ingrowth of cells. Some NSAIDs-based colon DDS, not selective for COX-2, such as aspirin or indomethacin, loaded into eFMs have been proposed, but its effectiveness in inflammation environments has not yet been demonstrated [17,19].

Considering these evidences, in this work we proposed a new DDS based on ETX-loaded eFMs for local delivery in the colorectal environment, overcoming the limitations associated with the systemic administration of ETX. This DDS can be placed in the inflamed region of the colon through colonoscopy or in the staple line after colorectal resection surgery followed by anastomosis. For its development, a range of ETX-loaded eFMs were produced and characterized morphologically, chemically, mechanically, and thermally. The release profile of different ETX concentrations loaded into eFMs was also studied. All the conditions were tested against epithelial and fibroblastic colon cell lines to demonstrate their cytocompatibility. Furthermore, the DDS loaded with the highest concentration of ETX was also tested against an immune cell model (i.e. human monocyte-derived macrophages cells) simulating an inflammatory environment.

2. Materials and methods

2.1. Materials

Polycaprolactone (PCL; Mw = 70,000–90,000 determined by GPC), chloroform, *N*,*N*-dimethylformamide (DMF), etoricoxib VETRANAL™ analytical standard, Phorbol 12-myristate 13-acetate (PMA), and Lipopolysaccharide (LPS) from *Escherichia coli* were purchased to Sigma-Aldrich. CellTiter 96® AQueous One Solution was purchased to Promega Corporation. Human colon epithelial (CCD 841 CoN; CRL-1790) and fibroblastic (CCD-18Co; CRL-1459) cells lines and Eagle's Minimum Essential Medium (EMEM) were purchased to the American Type Culture Collection. Fetal bovine serum (FBS), antibiotic antimycotic solution, and TrypLE™ Express with Phenol Red were purchased from Life Technologies Europe BV. Roswell Park Memorial Institute (RPMI) 1640 medium modified with GlutaMax™, Phenol Red, HEPES, Calcein AM dye and propidium iodide were purchased to Thermo Fisher Scientific. Human Monocytic Leukaemia cells (THP-1 cell line) were purchased to the European Collection of Authenticated Cell Cultures (ECACC). Prostaglandin E2 Parameter Assay Kit, Human IL-8/CXCL8 DuoSet enzyme-linked immunosorbent assay (ELISA), Human TNF-α DuoSet ELISA and DuoSet ELISA Ancillary Reagent Kit 2 were purchased to R&D Systems. Rhodamine phalloidin was purchased from Cytoskeleton, Inc. DAPI (4′,6-diamidino-2-phenylindole, dilactate) was purchased from Biotium, Inc.

2.2. Production of ETX-loaded eFMs

The production of PCL eFMs was performed as described elsewhere [20]. Briefly, a 20 % (*w/v*) PCL solution was prepared using an organic mixture of chloroform and DMF at an 8:2 volume ratio. After the complete dissolution of PCL, 1 mL of the solution was electrospun at 15.5 kV, using a needle tip-to-ground collector distance of 20 cm, and a flow rate of 1.0 mL h^{-1}. Then, the eFMs were allowed to dry for 1 day. For the preparation of ETX-loaded eFMs, ETX was dissolved in the polymeric solution at three concentrations (1, 2, and 3 mg mL^{-1}) and electrospun as described above.

2.3. Morphological characterization of ETX-loaded eFMs

The unloaded eFM and the ETX-loaded eFMs, i.e. eFMs loaded with 1, 2 and 3 mg mL^{-1} of ETX (eFM-ETX1, eFM-ETX2, and eFM-ETX3, respectively) were coated with gold using a Sputter Coater (Cressington, model 108 A). Then, the morphology of the samples was characterized using a scanning electron microscope (SEM) (JEOL, model JSM-6010 LV). At least 9 micrographs of each condition were recorded to determine the fiber diameter and pore size using *ImageJ* (version 1.52). The porosity was calculated using the median values of fiber diameter and pore size for each micrograph according to the following formula [21]:

$$\text{Porosity}\ (\%) = e^{-\frac{\text{fiber diameter}}{\text{pore size}}} \times 100$$

2.4. Mechanical characterization of ETX-loaded eFMs

The mechanical properties (i.e., tensile modulus, maximum tensile strength, and strain at break) of unloaded eFM and ETX-loaded eFMs were determined. For that, uniaxial tensile tests using a Universal Mechanical Testing Equipment (INSTRON, model 5543) equipped with a 50 N load cell at crosshead speed of 2 mm min^{-1} and a 10 mm gauge length were used. Strips (18 mm × 5 mm) of the different eFMs conditions were prepared and fixed in paper frames to keep the dimensional stability of the specimens. The specimens presented approximately 200 μm of thickness and were tested under dry conditions, and at room temperature. Before testing, the lateral sides of the paper frames were cut to allow to monitor the correct deformation of the specimens. The mechanical tests were performed until complete fracture of the specimens. At least 9 specimens from different batches of each condition were tested.

2.5. Thermal characterization of ETX-loaded eFMs

The thermal properties (i.e., onset temperature, peak temperature, variation of enthalpy and crystallinity percentage) for both melting and crystallization processes of unloaded eFM and ETX-loaded eFMs were determined using Differential Scanning Calorimetry (DSC) (T. A. INSTRUMENTS, model DSC Q100). For that, 3 samples from different batches of each condition with approximately 4.5 mg were packed into aluminium pans, heated at a constant rate of 10 °C min^{-1} over a temperature range of 0 to 180 °C, and then cooled down to 0 °C at the same temperature rate. An inert atmosphere was maintained by purging nitrogen gas at a flow rate of 50 mL min^{-1}. For the determination of crystallinity, the following formula [22] was used:

$$\text{Crystallinity}\ (\%) = \frac{\text{Melting Enthalpy of PCL}}{\text{Melting Enthalpy of Fully Crystalline PCL}} \times 100$$

The melting enthalpy of fully crystalline PCL was considered 139.5 J/ g [22]. When samples contained ETX, this value was multiplied by the weight fraction of PCL present in each condition.

2.6. Chemical characterization of ETX-loaded eFMs

Samples analysis was performed on a Kratos Axis-Supra instrument with ESCApe software and equipped with a monochromatized radiation

X-ray source of aluminium Kα (Al-Kα, 1486.6 eV). Samples were placed on a sample holder further localized perpendicularly to the radiation source under a vacuum atmosphere (10^{-8} Pa). The chemical composition of the samples surface was assessed using a 15 mA emission current and a pass energy of 160 eV for survey and 20 eV for high resolution regions analysis. The regions spectra of C 1s and O 1s, for unloaded eFM and additionally N 1s and S 2p for eFMs-ETX samples were performed using a linear type background fitting. Charge referencing was performed for the C1s hydrocarbon peak, which was set at 285.0 eV. Each sample was analysed at three different locations in quintuplicate, being the presented data a media of all the achieved results for each composition.

2.7. In vitro drug release study

The release of ETX from the different eFMs conditions was studied using 3 disks from different batches with 20 mm diameter. For that, the eFMs were immersed in 10 mL of 0.9 % (*w/v*) NaCl solution at pH 7.4. The release study was conducted at 37 °C and 60 rpm for 168 h using an orbital shaker (IKA, model KS 260 control). At defined time points (0.5, 1, 2, 3, 4, 5, 6, 7, 8, 9, 10, 11, 12, 22, 24, 26, 28, 30, 32, 34, 36, 48, 52, 56, 60, 72, 96, 120, 144, and 168 h), an aliquot of 1 mL was collected and replaced with fresh NaCl solution. The absorbance was measured using a microplate reader (BioTEK, model Synergy HT) at 234 nm. To determine the ETX concentration of each sample, a calibration curve of known ETX concentrations was used. In the calculations, the absorbance of unloaded eFM in the same release medium at each time point was subtracted from the values of all ETX-loaded eFMs conditions.

2.8. Cytocompatibility evaluation of the ETX-loaded eFMs

Two human colon cell lines with epithelial and fibroblastic morphology (i.e., CCD 841 CoN and CCD-18Co, respectively) were used to evaluate the cytocompatibility of unloaded eFM and ETX-loaded eFMs. All conditions of eFMs samples were performed with 5 mm squares. Tissue culture polystyrene (TCP) coverslips were used as a control. All conditions were performed at least in triplicate and assayed at least 3 times independently. The experiments were performed according to a procedure described elsewhere [20].

2.8.1. Cell culture and seeding

Both cell lines, at passages 13–16, were grown in EMEM supplemented with 10 % (*v/v*) of FBS and 1 % (v/v) of antibiotic antimycotic solution, at 37 °C in a humidified atmosphere of 5 % CO_2. For the cell seeding, 50,000 cells resuspended in a droplet were seeded over each sample and allowed to adhere for 4 h. After this time, culture medium was added.

2.8.2. Metabolic activity

The metabolic activity of human colonic cells seeded on all eFMs conditions and TCP was determined by MTS assay. After 1, 3, and 7 days of culture, the medium was removed and the samples were rinsed with Dulbecco's phosphate-buffered saline (DPBS). After that, a mixture of DMEM without phenol red with 1 % (*v/v*) of antibiotic antimycotic solution and MTS reagent (5:1 volume ratio) was added to each well and left to incubate for 3 h at 37 °C in a humidified 5 % CO_2 atmosphere. For the negative control, wells without cells or samples were used. The absorbance of the MTS reaction medium from each sample was read in triplicate at 490 nm (BioTEK, model Synergy HT).

2.8.3. Live/dead assay

Live/Dead assay was performed after 1, 3, and 7 days of culture. For that, living cells were stained with 2 μg mL^{-1} calcein AM (green) and dead cells with 1 μg mL^{-1} propidium iodide (red). After that, the stained cells were observed in an AiryScan 2 confocal microscope (Zeiss, model LSM 980).

2.8.4. Morphological characterization

After 1, 3, and 7 days of culture, the medium was removed, and the samples were washed with PBS. Then, they were fixed with 10 % buffered formalin for 1 h at 4 °C. To observe the cell morphology, the cytoskeleton and the nucleus were stained with phalloidin-TRITC (1:200) and DAPI (1:500), respectively, and imaged in an AiryScan 2 confocal microscope (Zeiss, model LSM 980).

2.9. Anti-inflammatory evaluation of the ETX-loaded eFMs

A human peripheral blood monocyte cell line (THP-1) was used to evaluate the anti-inflammatory capacity of unloaded eFMs and loaded with the highest concentration of ETX (i.e., eFM-ETX3). All condition samples were performed with 10 mm size squares in triplicate and assayed 3 times independently. The experiments were performed according to a procedure described elsewhere [23] with some modifications.

2.9.1. Cell culture and seeding

The THP-1 cells were grown in RPMI 1640 medium with GlutaMAX™ and HEPES, supplemented with 10 % (*v/v*) of FBS and 1 % (v/v) of antibiotic antimycotic, and maintained at 37 °C in a humidified atmosphere of 5 % CO_2. The cells were seeded in a 24-well culture plate at a density of 5×10^5 cells per well, and their differentiation was induced by adding 1 mL of RPMI medium containing 100 nM PMA per well for 24 h. After that, the medium was removed, the adherent cells were washed with warm RPMI medium, and then incubated for 48 h with 1 mL of RPMI medium (without PMA to ensure the complete differentiation of monocyte to macrophage phenotype). After this time, the medium was removed and the macrophages were stimulated with RPMI medium containing 100 ng mL^{-1} of LPS for 24 h. As negative control of the inflammatory stimulus, cells without LPS stimulation were used. After the inflammatory stimulus, eFM and eFM-ETX3 samples were added to the LPS-stimulated macrophages and incubated for 1 and 3 days. These time points were defined considering the release profile of ETX.

2.9.2. Metabolic activity

The metabolic activity of THP-1 cells adhered on the well or on the eFMs was determined by MTS assay. After 1 and 3 days, the culture medium was removed and the samples were rinsed with warm DPBS. The remain procedure was conducted as described in Section 2.8.2.

2.9.3. Quantification of pro-inflammatory molecules

The amount of PGE_2, IL-8, and TNF-α was quantified by ELISA according to the manufacturer's instructions. Briefly, in the case of PGE_2 quantification, samples, controls, or standards were added to each well followed by the addition of the primary antibody solution. After an incubation of 1 h at room temperature under agitation, the secondary conjugated antibody solution was also added and incubated for another 2 h on the shaker. Afterwards, the plate was washed, and the substrate solution was added. After 30 min, the stop solution was added and the optical density was read at 450, 540, and 570 nm (BioTEK, model Synergy HT). For IL-8 and TNF-α quantification, the capture antibody was added to each well and incubated overnight at room temperature. The block buffer was added and incubated for 1 h. Then, the samples or standards were added and followed by the detection antibody. In each of these steps, a 2 h incubation was performed. After that, the Streptavidin-HRP and substrate solution were added (20 min incubation each). Afterward the stop solution was added, and the plate read as described above. Except between the addition of substrate and stop solutions, washes were performed between each step. For PGE_2, IL-8, and TNF-α, absorbance readings at 540 or 570 nm were subtracted from readings at 450 nm to correct for plate imperfections. Standard curves were constructed with known concentrations ranging from 39 to 2500 pg mL^{-1} for PGE_2, 31.3 to 2000 pg mL^{-1} for IL-8, and 15.6 to 1000 pg mL^{-1} for

TNF-α, and the concentration of each sample was calculated from these standard curves.

2.10. Statistical analysis

Statistical analysis was performed using Graph Pad Prism Software. The data were first tested using the Shapiro-Wilk normality test. Differences between the different conditions were analysed using nonparametric tests (Kruskal–Wallis or Mann-Whitney tests), and $p <$ 0.05 was considered significant. When multiple comparisons were performed, the Dunn's test was used.

3. Results

3.1. Morphology of the ETX-loaded eFMs

The eFMs were loaded with different concentrations of ETX and characterized by SEM. The morphology of the different conditions was

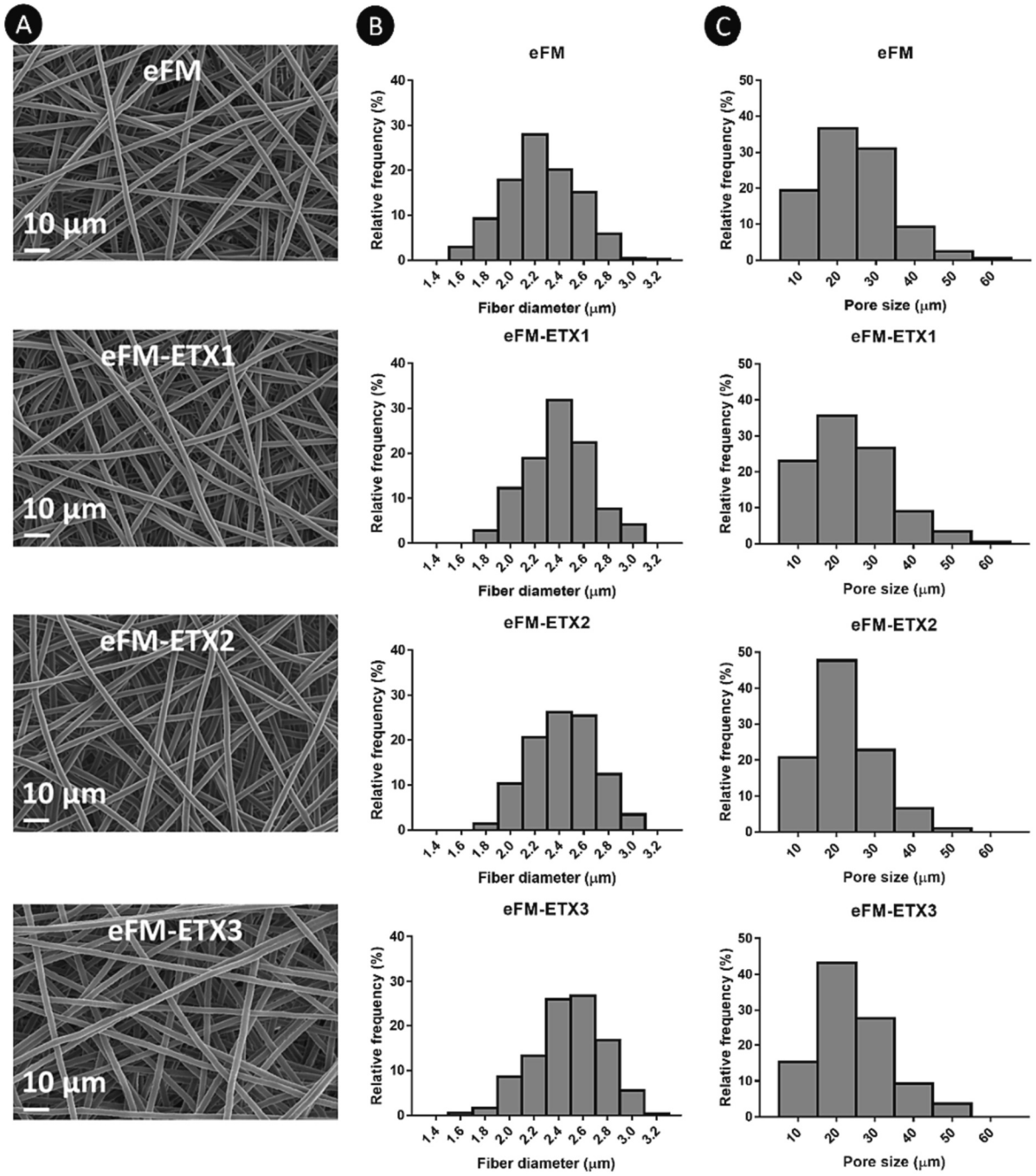

D

	eFM	eFM-ETX1	eFM-ETX2	eFM-ETX3
Porosity (%)	90.59 (89.40-91.43)	89.83 (88.02-90.64)	89.79 (88.45-90.40)	89.54 (88.43-90.09)

Fig. 1. Morphological characterization of eFM, eFM-ETX1, eFM-ETX2, and eFM-ETX3: (A) SEM micrographs; (B) fiber diameter; (C) pore size; (D) porosity - data are presented as median ± interquartile range (i. q. r.).

similar, even after loading of the ETX (Fig. 1A). All eFMs conditions presented a homogeneous morphology composed of randomly oriented fibers. Looking at the relative frequency of fiber diameter, it was found that loading the eFMs with ETX promoted an increase in fiber diameter (Fig. 1B). On the other hand, no significant differences were found regarding pore size (Fig. 1C). All eFMs conditions exhibit high porosity (median values between 89.54 and 90.59 %), with no significant differences between conditions (Fig. 1D).

3.2. Mechanical properties of the ETX-loaded eFMs

Representative stress-strain curves for unloaded eFMs and loaded with different concentrations of ETX are presented in Fig. 2A. The mechanical properties, i.e., tensile modulus, maximum strength, and the strain at break, are represented in Fig. 2B. The tensile modulus and maximum strength of the unloaded eFM were 18.08 (15.26–21.24) MPa and 4.21 (2.97–4.69) MPa, being 12.33 (9.76–15.03) MPa and 3.22 (2.73–3.94) MPa for ETX-loaded eFMs, respectively. For the strain at break of the produced eFMs, the median values were 1535 (1364–1631) % for all the tested conditions. No significant differences were found between conditions for all these properties.

3.3. Thermal properties of the ETX-loaded eFMs

Representative DSC thermograms of unloaded eFMs and loaded with different concentration of ETX are presented in Fig. 3. DSC data of each endothermic and exothermic transition for all conditions are detailed in Table 1. No major differences were found between conditions for the melting and crystallization peak temperatures, and crystallinity for both endothermic and exothermic transitions. Only a significant decrease on the enthalpy (~7 °C) on the endothermic transition was observed for the eFM loaded with the highest concentration of ETX (i.e., eFM-ETX3) when compared with the unloaded eFMs.

3.4. Chemical composition of the ETX-loaded eFMs

The ETX-loaded eFMs were analysed by X-ray photoelectron spectroscopy (XPS) and shown in Fig. 4A. From the XPS high resolution spectra, the atomic ratios (at.%) of C, O, S, and N on the surface of the eFMs were determined (Fig. 4B). On eFMs loaded with ETX at different concentrations were noticed the appearance of additional peaks related to nitrogen and sulphur as expected (Fig. 4C), inexistant for unloaded eFM. They confirmed the presence of ETX on the fibrous structure, although at reduced amounts (Fig. 4B).

3.5. Drug release profile of the ETX-loaded eFMs

The release profile of the ETX loaded into eFMs at different concentrations was evaluated using 0.9 % NaCl as release solution at 37 °C and 60 rpm, to mimic physiological conditions. The profile showed a burst release of ETX in the first 12 h, followed by a rapid release until 36 h (Fig. 5). After that time, the release was slower up to 60 h, accompanied by a gradual and sustained release until the end of the study. These differences were more pronounced as the concentration of ETX loaded into eFMs increased.

3.6. Cytocompatibility of the ETX-loaded eFMs in the presence of colonic cells

The metabolic activity of human colon epithelial (CCD 841 CoN cell line) and fibroblastic (CCD-18Co cell line) cells seeded on TCP, unloaded eFMs and loaded with different concentration of ETX was determined along 7 days. The results showed that, an increase in the concentration of ETX did not significantly affect the metabolic activity of both colonic cell types when compared to unloaded eFMs (Fig. 6A and B). To confirm visually the cells viability, a Live/Dead assay was conducted, whose results are presented in Supplementary Fig. 1A and B. The

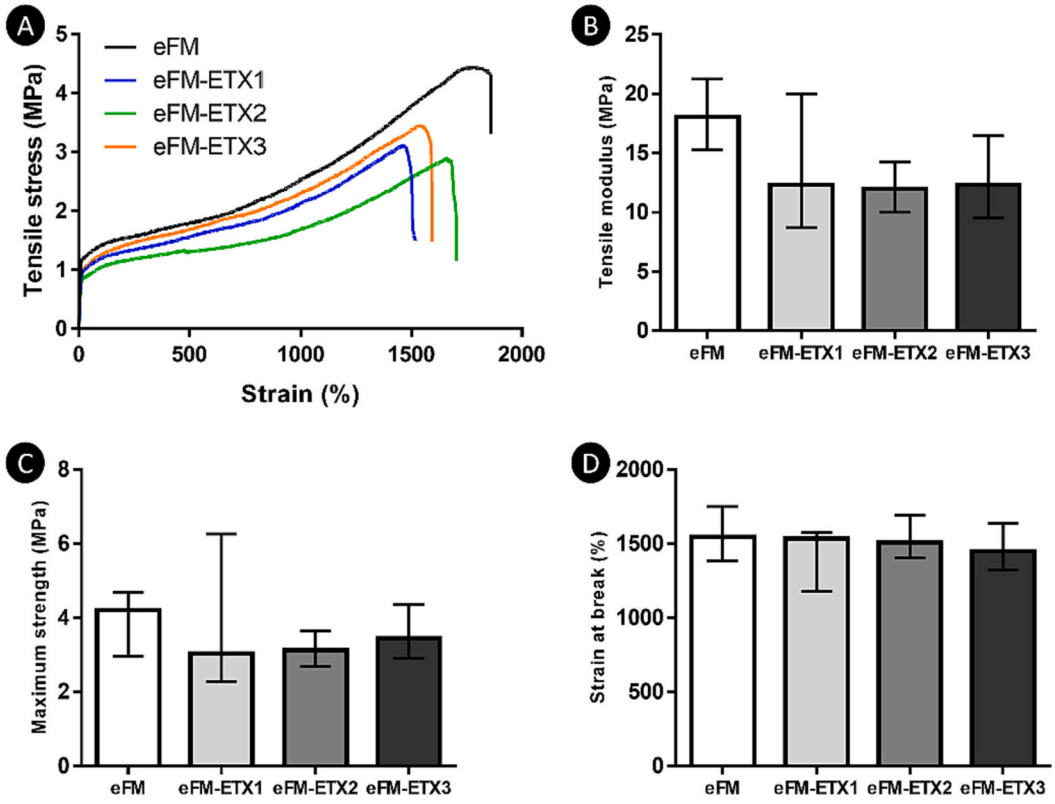

Fig. 2. Mechanical characterization of eFM, eFM-ETX1, eFM-ETX2, and eFM-ETX3: (A) representative stress-strain curves; (B) tensile modulus; (C) maximum strength; (D) strain at break. Data are presented as median ± i. q. r. Results were considered statistically significant at $p < 0.05$.

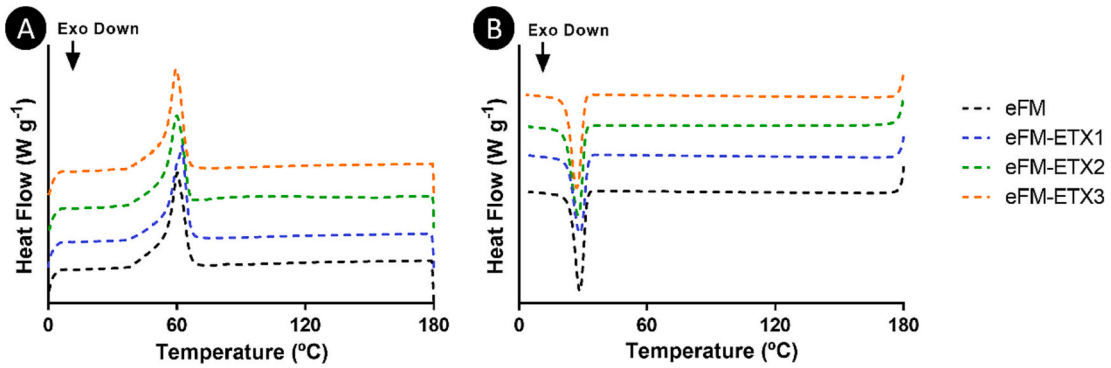

Fig. 3. Representative DSC thermograms of eFM, eFM-ETX1, eFM-ETX2, and eFM-ETX3: (A) heating cycle or endothermic transition; (B) cooling cycle or exothermic transition.

Table 1
DSC data of eFM, eFM-ETX1, eFM-ETX2, and eFM-ETX3 for endothermic and exothermic transitions. Data are presented as median ± i. q. r. Results were considered statistically significant at $p < 0.05$ (*).

Sample	1st Heating		Cooling		Crystallinity (%)
	Melting peak temperature (°C)	Variation of enthalpy (J/g)	Crystallization peak temperature (°C)	Variation of enthalpy (J/g)	
eFM	60.24 (59.51–60.47)	74.48 (73.08–77.47)	28.64 (24.45–29.66)	60.63 (59.80–61.05)	43.46 (42.87–43.76)
eFM-ETX1	60.22 (56.72–60.76)	69.87 (69.83–70.27)	27.61 (26.05–28.66)	55.76 (55.33–60.74)	40.17 (39.86–43.76)
eFM-ETX2	56.54 (56.36–59.93)	70.95 (68.19–72.45)	27.94 (26.62–28.47)	60.26 (60.24–61.21)	43.63 (43.62–44.32)
eFM-ETX3	56.68 (56.31–59.92)	67.18 (66.86–69.61)*	28.12 (25.55–28.61)	58.06 (55.25–58.10)	42.25 (40.21–42.28)

morphological characterization showed that adherent epithelial and fibroblastic cells (Fig. 7A and B, respectively), in the 1st day, tend to aggregate when cultured in the eFMs-based conditions, as compared to the spread phenotype in TCP. Along time, both colonic cells tend to acquire a spread morphology. Based on all previous results, the eFM condition loaded with the highest concentration of ETX (i.e., eFM-ETX3) was used in subsequent tests.

3.7. Cytocompatibility and anti-inflammatory activity of ETX-loaded eFMs in the presence of immune cells

The anti-inflammatory activity of unloaded eFMs and loaded with the highest concentration of ETX (i.e., eFM-ETX3) was evaluated at different time points (1 and 3 days) using human peripheral blood monocytes (THP-1 cell line) differentiated into macrophages and further stimulated with LPS. When the macrophages were not stimulated with LPS, their metabolic activity was significantly reduced (Fig. 8). The metabolic activity of stimulated macrophages significantly increased when eFMs was added to the culture medium, being this increase higher in ETX-loaded eFMs.

The secretion of PGE_2, IL-8, and TNF-α was quantified to ascertain about the anti-inflammatory properties of unloaded eFMs and loaded with the highest concentration of ETX (i.e., eFM-ETX3). The results demonstrated that the ETX released from eFM promotes a statistically significant reduction in the percentage of both PGE_2 and IL-8 ($p = 0.0476$, when comparing the positive control with LPS stimulation + eFM-ETX3 condition) (Fig. 9). Concerning TNF-α, both LPS stimulation + eFM and LPS stimulation + eFM-ETX3 conditions significantly reduced the percentage of TNF-α comparing with the positive control ($p = 0.0022$), despite a tendency towards lower values with the LPS stimulation + eFM-ETX3 condition.

4. Discussion

Selective COX-2 inhibitors are potentially indicated for many of the inflammatory disorders that can affect the intestinal region. Although ETX has been used for analgesic and anti-inflammatory purposes [10–12], major concerns still arise (i.e. cardiovascular toxicity) regarding its non-specific action. Therefore, the development of DDS targeting the colon is still a medical need. Some authors [24] proposed eFMs containing pectin and time-dependent polymers aimed for colonic drug delivery of another selective COX-2 inhibitor, i.e. celecoxib, but the results were limited to the preparation and characterization of the system, and dissolution studies. So far, ETX-based DDS have been proposed for pain management and osteoarthritis [25–27], being colon-targeted DDS not reported yet. In contrast to the reported DDS, eFMs become promising and versatile because, in addition to presenting encapsulation efficiency rates near to 100 %, they are easily adaptable to the colonic tissue. Therefore, they allow the release of the loaded drug directly at the implantation site, avoiding migration and off-site action, also benefiting from its high surface area and porosity. The drug release profile can be further controlled by varying the drug and polymer ratio, fiber diameter and morphology through a simple and cost-effective process [28,29].

Accordingly, this study proposes a new DDS based on eFMs loaded with ETX for intestinal disorders. Increasing the concentration of ETX promotes an increase in the eFMs fiber diameter, as expected, although no changes were observed regarding pore size and porosity, important features to allow cells ingrowth. The mechanical characterization under tensile load of the eFM showed higher stiffness and tensile strength when compared with the ETX-loaded eFMs, however no significant differences were found between conditions. The mechanical properties of the ETX-loaded eFMs also demonstrated that the drug amount did not promote significant changes in the tensile modulus, maximum strength, and strain at break. These results are in agreement with the similar morphology of the eFMs observed by SEM analysis. In addition, all the produced eFMs presented a ductile behaviour showing a maximum strain higher than 1000 %. Other authors [30], reporting PCL/PEG nanofibers, demonstrated that the addition of ibuprofen (another NSAID) caused a decrease in maximum stress and an increase in the percentage of maximum strain. Regarding the thermal stability of eFMs, it has been reported that neat PCL showed an endothermic peak around 67 °C [26,31]. By other side, pure ETX displays a sharp and endothermic peak at 139.2 °C [26,32]. In the thermograms of the different ETX-

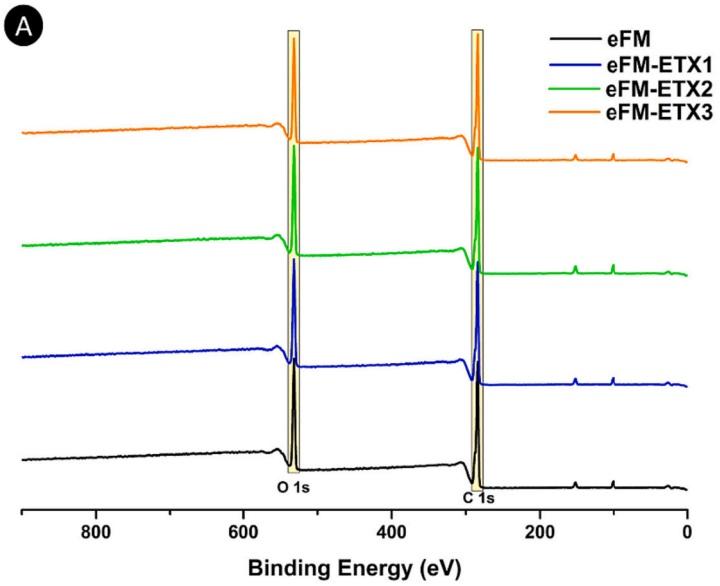

B

	C 1s	O 1s	N 1s	S 2p
eFM	77.49 ± 0.19	22.51 ± 0.19	-	-
eFM-ETX1	77.09 ± 0.22	22.42 ± 0.19	0.15 ± 0.14	0.10 ± 0.03
eFM-ETX2	77.22 ± 0.22	21.96 ± 0.19	0.39 ± 0.14	0.13 ± 0.04
eFM-ETX3	77.48 ± 0.22	21.92 ± 0.19	0.43 ± 0.16	0.15 ± 0.03

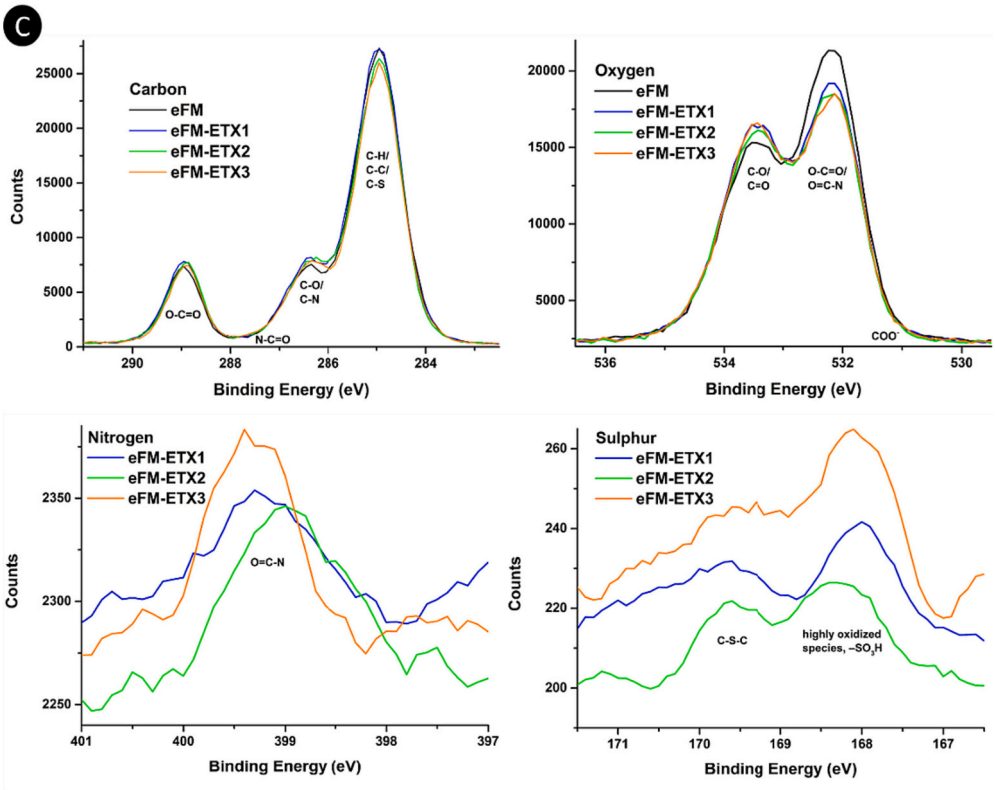

Fig. 4. XPS analysis of eFM, eFM-ETX1, eFM-ETX2, and eFM-ETX3: (A) wide scan; (B) elemental composition (% C, N, O and S) derived from high resolution spectra - data are presented as average ± SD; (C) C 1s, O 1s, S 2p and N 1s region scans.

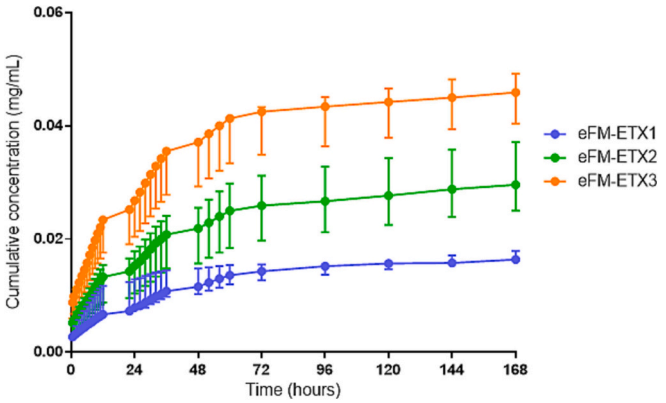

Fig. 5. Cumulative release of the different ETX concentrations from eFMs. Data are presented as median ± i. q. r.

loaded eFMs, the peak related to the melting point of ETX was absent, being only observed the peak assigned to PCL. This finding suggests that the drug ETX was dissolved or molecularly dispersed into the PCL matrix in its amorphous form [26], seeming to corroborate the results obtained in the system mechanical characterization since no significant differences were observed in the crystallinity.

The incorporation of ETX presented no significant changes in the high-resolution XPS regions of C1s and O1s spectra, suggesting the absence of significant chemical bounds between the drug and the polymer (i.e. PCL). According to these findings, a drug entrapment into the fibers may be supported through physical (not chemical) interactions between the ETX and the PCL matrix. The ETX functional groups were detected through S 2p and N 1s regions spectra. Their relative content in the fibers is proportional to the amount of incorporated drug, increasing from ETX1 to ETX3.

Since the proposed DDS is intended to be applied locally at the inflamed colonic environment, it will not be subjected to gastric environment. Therefore, the *in vitro* drug release study was conducted in a 0.9 % NaCl solution at 37 °C and at pH 7.4 to simulate the mild alkaline conditions of the colon [33]. The results obtained demonstrate that almost all the drug was released within the first 60 h, with a release rate consistent with the concentration of ETX loaded into the eFMs. The proposed DDS demonstrated to have a faster release profile than other ETX-based [25,26]. The short release time address the local, non-systemic action of this DDS, requiring more efficient action in the first days. Furthermore, this allows ETX to act in the acute phase of the inflammation after intestinal surgeries, being maintained until at least the onset of collagen synthesis (168 h) [34]. Indeed, in the treatment of IBD, it is important to have an initial inhibition of the inflammatory state and then a maintenance phase where the drug will control the disease [35].

Being this DDS intended for a local application at the colon, understanding the cellular response to the ETX-loaded eFMs is essential to ensure its safety. The cytocompatibility evaluation demonstrate that all the ETX concentrations did not promote changes in cell viability. In addition, no changes were also observed in the morphology of both endothelial and fibroblastic colonic cells. This result is specially promising since the local delivery of ETX will not affect the colorectal cellular environment, allowing to overcome the problems related with its systemic administration and also reducing the quantity of drug administered to the patients for having the intended therapeutic effect.

Besides the colonic cells, macrophages are also key players at the colorectal environment, performing different roles in various intestinal diseases. They are associated with the development of a response to intestinal inflammation by the secretion of cytokines and bioactive substances [36–38]. Furthermore, it is also known that elevated quantities of LPS have been linked to intestinal inflammation in IBD conditions, promoting a cascade of inflammatory pathways [39]. Taking this into consideration, the inflammatory scenario of the colon was simulated by an *in vitro* activation of human macrophages with LPS. The metabolic activity of stimulated macrophages increased in the presence of an external stimulus, namely when eFMs were added to the culture. When the highest concentration of ETX was loaded into eFMs (i.e., eFM-ETX3), the released drug has an effect over the macrophages, increasing their metabolic activity. Therefore, the proposed DDS at the highest concentration, in addition to demonstrated cytocompatibility with human epithelial and fibroblastic colonic cells, also did not compromise the viability of immune cells.

COX-2 is upregulated by inflammatory cytokines, catalyzing the production of PGs associated with pathological situations, including IBD

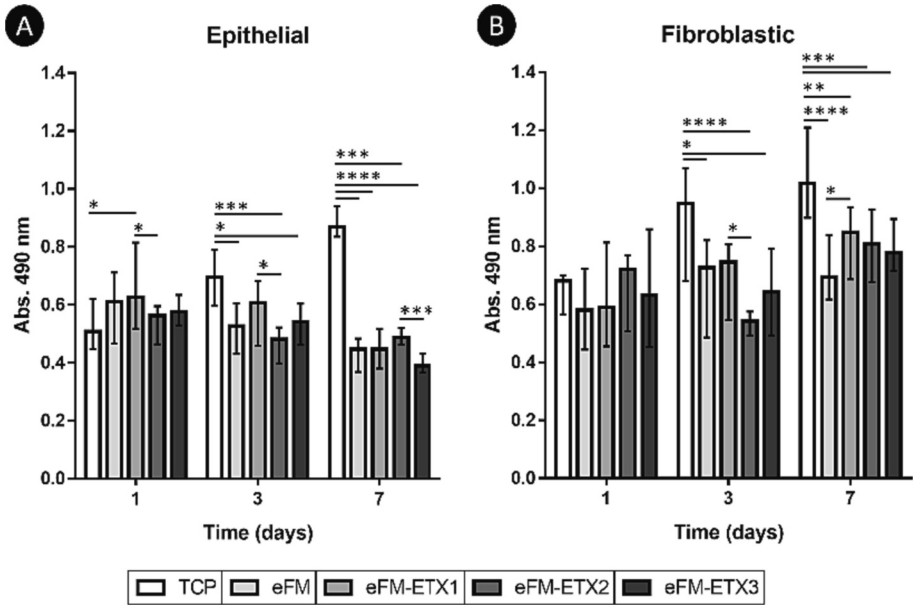

Fig. 6. Metabolic activity of human colonic cells cultured on TCP, unloaded eFMs and loaded with different concentration of ETX along 7 days: (A) epithelial CCD 841 CoN; (B) and fibroblastic CCD-18Co cell lines. Data are presented as median ± i. q. r. Results were considered statistically significant at $p < 0.05$ (*); ** $p < 0.01$; *** $p < 0.001$; and **** $p < 0.0001$.

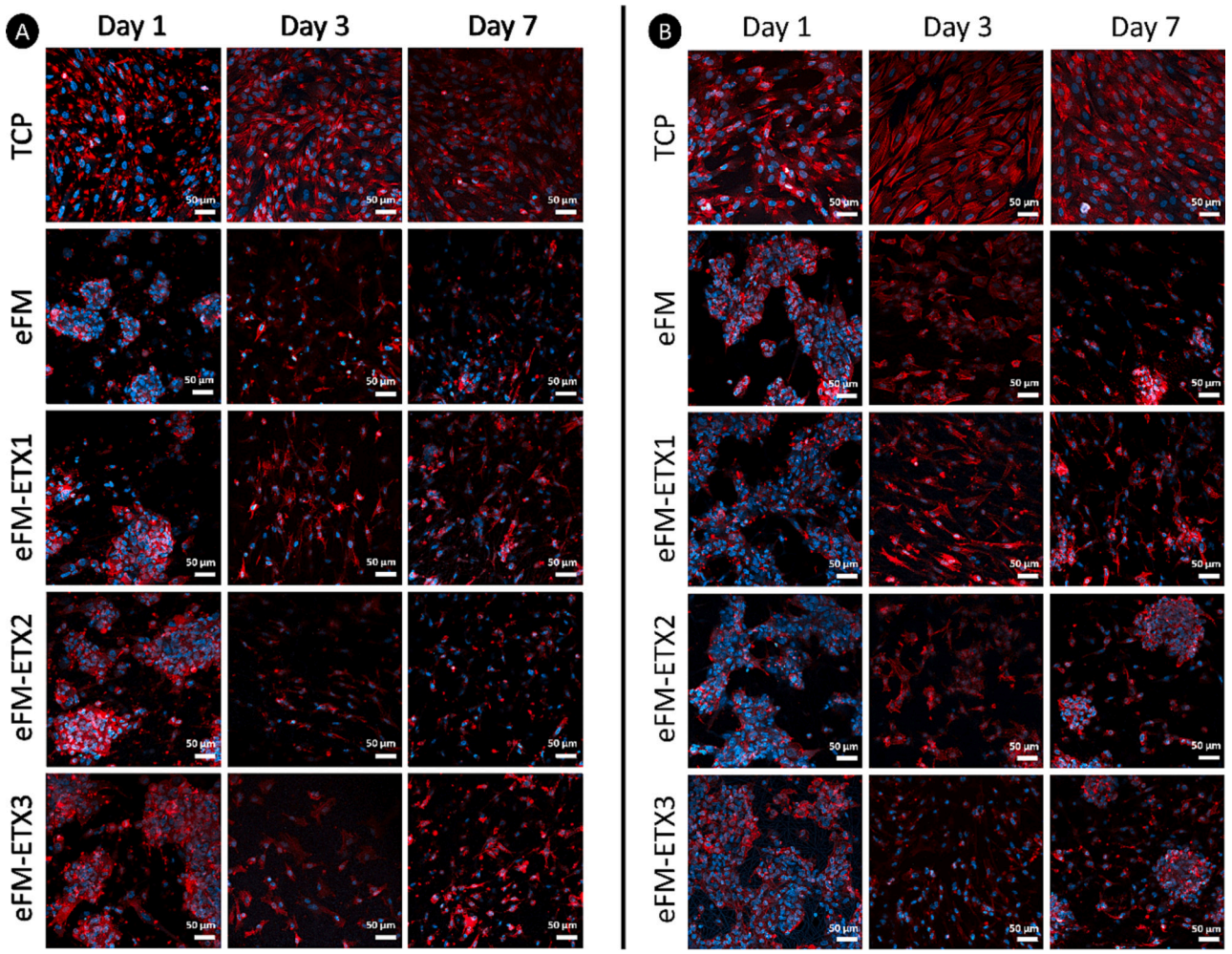

Fig. 7. Representative fluorescence microscopy images showing the morphology of human colonic cells cultured on TCP, unloaded eFMs and loaded with different concentration of ETX along 7 days, with the cytoskeleton in red and nucleus in blue: (A) epithelial CCD 841 CoN; (B) and fibroblastic CCD-18Co cell lines.

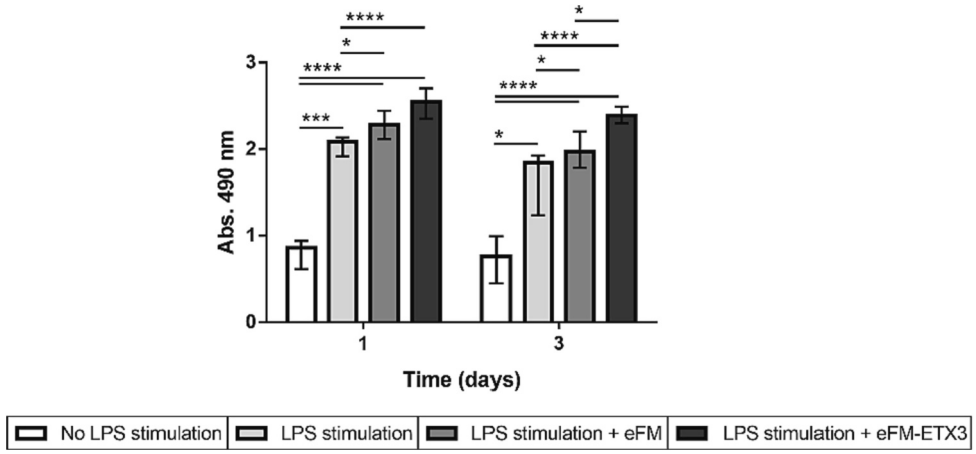

Fig. 8. Metabolic activity of THP-1 monocytes differentiated into macrophages, stimulated or not with LPS, and cultured in the presence of unloaded eFM or eFM-ETX3 along time points (1 and 3 days). Data are presented as median ± i. q. r. Results were considered statistically significant at $p < 0.05$ (*); *** $p < 0.001$; and **** $p < 0.0001$.

and colorectal cancer [4–7]. It is, therefore, important to understand if the proposed DDS interferes with PGE_2 levels, a PG that mediates the proinflammatory and tumour-promoting effects of COX-2 in such disorders [40]. The results obtained demonstrated that the eFM loaded with ETX at the highest concentration (i.e., eFM-ETX3) promotes a statistically significant reduction in the percentage of PGE_2. Complementarily, the potential of DDS was also confirmed by a reduction in the percentage of IL-8, another cytokine involved in the inflammatory processes promoted by COX-2 [41]. The results obtained for TNF-α also demonstrated that ETX-loaded eFM also present a considerable anti-

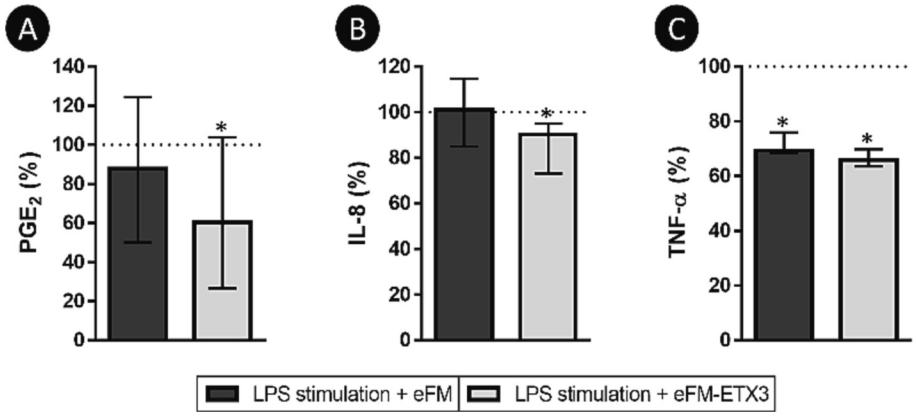

Fig. 9. PGE_2 (A), IL-8 (B), and TNF-α (C) secreted by LPS-stimulated macrophages cultured in the presence of unloaded eFM and eFM-ETX3 after 1 day. The dotted line represents the positive control of the assay (LPS-stimulated macrophages alone). Data are presented as median ± i. q. r. Results were considered statistically significant at $p < 0.05$ (*).

inflammatory activity. This reduction in the TNF-α percentage is a promising finding given that TNF-α signalling has been reported to play a critical role, not only in the pathogenesis of IBD, but also in infectious diseases, in the healing of intestinal wounds and in the formation of tumors [42]. All together, these results demonstrate and support the potential use of the proposed DDS in the treatment of intestinal inflammatory diseases.

5. Conclusions

eFMs with different concentrations of a selective COX-2 inhibitor, i.e. ETX, were successfully produced, for the first time with a random morphology and dimensional stability, aiming intestinal inflammatory disorders. The presence of ETX into the eFMs was confirmed through the identification of the nitrogen and sulphur elements by XPS, although not compromising the morphology and mechanical stability of the eFMs. The ETX present a burst release in the first 12 h followed by a fast release until the 36 h, and a gradual decreased until the end of the study. Importantly, the different concentrations of ETX loaded into the eFMs were not toxic to human colonic cells. When the highest concentration of ETX loaded into the eFMs was tested for the anti-inflammatory activity, the immune cells viability was not compromised, while promoting a significant reduction in the percentage of secreted PGE_2, IL-8 and TNF-α. Therefore, the proposed DDS may be a promising approach to control inflammatory disorders associated with COX-2 in colorectal diseases.

Supplementary data to this article can be found online at https://doi.org/10.1016/j.bioadv.2023.213712.

CRediT authorship contribution statement

Ana Oliveira: Conceptualization, Methodology, Formal analysis, Investigation, Data curation, Writing – original draft, Writing – review & editing. **Luísa C. Rodrigues:** Formal analysis, Investigation, Data curation, Writing – original draft, Writing – review & editing. **Diana Soares da Costa:** Investigation, Data curation, Writing – review & editing. **Emanuel M. Fernandes:** Validation, Writing – review & editing. **Rui L. Reis:** Resources, Writing – review & editing, Funding acquisition. **Nuno M. Neves:** Writing – review & editing, Supervision. **Pedro Leão:** Writing – review & editing, Supervision. **Albino Martins:** Conceptualization, Methodology, Validation, Resources, Writing – review & editing, Supervision, Project administration.

Declaration of competing interest

The authors declare that they have no known competing financial interests or personal relationships that could have appeared to influence the work reported in this paper.

Data availability

Data will be made available on request.

Acknowledgements

The authors thank the Portuguese Foundation for Science and Technology (FCT) and CUF, S.A. for the Ph.D. scholarships of A. Oliveira (PD/BDE/142979/2018 and COVID/BDE/152779/2022). The authors also thank the FCT for the financial support of L. C. Rodrigues (SFRH/BPD/93697/2013), D. Soares da Costa (SFRH/BPD/85790/2012) and the projects UIDB/50026/2020, and UIDP/50026/2020. This work was also financially supported by the project Bluebiolab – Transboundary Marine Biotechnology Laboratory (0474_BLUEBIOLAB_1_E) financed by the Interreg programme Spain-Portugal through the European Regional Development Fund (ERDF). Furthermore, the authors would like to thank the contributions to this research from the project TERM RES Hub – Scientific Infrastructure for Tissue Engineering and Regenerative Medicine, reference PINFRA/22190/2016 (Norte-01-0145-FEDER-022190), funded by FCT in cooperation with the Northern Portugal Regional Coordination and Development Commission (CCDR-N), for providing relevant lab facilities, state-of-the art equipment and highly qualified human resources.

References

[1] N.A. Nasef, S. Mehta, Role of inflammation in pathophysiology of colonic disease: an update, Int. J. Mol. Sci. 21 (13) (2020) 4748.
[2] K.W. Reisinger, M. Poeze, K.W. Hulsewé, B.A. van Acker, A.A. van Bijnen, A. G. Hoofwijk, J.H. Stoot, J.P. Derikx, Accurate prediction of anastomotic leakage after colorectal surgery using plasma markers for intestinal damage and inflammation, J. Am. Coll. Surg. 219 (4) (2014) 744–751.
[3] A. Oliveira, S. Faria, N. Gonçalves, A. Martins, P. Leão, Surgical approaches to colonic and rectal anastomosis: systematic review and meta-analysis, Int. J. Colorectal Dis. 38 (1) (2023) 52.
[4] D. Wang, C.S. Cabalag, N.J. Clemons, R.N. DuBois, Cyclooxygenases and prostaglandins in tumor immunology and microenvironment of gastrointestinal cancer, Gastroenterology 161 (6) (2021) 1813–1829.
[5] Y. El Miedany, S. Youssef, I. Ahmed, M. El Gaafary, The gastrointestinal safety and effect on disease activity of etoricoxib, a selective cox-2 inhibitor in inflammatory bowel diseases, Official journal of the American College of Gastroenterology|ACG 101 (2) (2006) 311–317.
[6] I.H.J.T. De Hingh, H. Van Goor, B.M. De Man, R.M.L.M. Lomme, R.P. Bleichrodt, T. Hendriks, Selective cyclo-oxygenase 2 inhibition affects ileal but not colonic anastomotic healing in the early postoperative period, Journal of British Surgery 93 (4) (2006) 489–497.
[7] C.H. Koehne, R.N. Dubois, COX-2 inhibition and colorectal cancer, in: Seminars in Oncology vol. 31, WB Saunders, 2004, pp. 12–21.
[8] D. Wang, R.N. DuBois, The role of anti-inflammatory drugs in colorectal cancer, Annu. Rev. Med. 64 (2013) 131–144.

[9] D.G. Ribaldone, S. Fagoonee, M. Astegiano, C. De Angelis, A. Smedile, G. P. Caviglia, E. Petrini, A. Greco, R. Pellicano, Coxib safety in patients with inflammatory bowel diseases: a meta-analysis, Pain Physician 18 (6) (2015) 599.
[10] I.G.E. Zarraga, E.R. Schwarz, Coxibs and heart disease: what we have learned and what else we need to know, J. Am. Coll. Cardiol. 49 (1) (2007) 1–14.
[11] N.G. Agrawal, A.G. Porras, C.Z. Matthews, E.J. Woolf, J.L. Miller, S. Mukhopadhyay, D.C. Neu, K.M. Gottesdiener, Dose proportionality of oral etoricoxib, a highly selective cyclooxygenase-2 inhibitor, in healthy volunteers, J. Clin. Pharmacol. 41 (10) (2001) 1106–1110.
[12] A.D. Rodrigues, R.A. Halpin, L.A. Geer, D. Cui, E.J. Woolf, C.Z. Matthews, K. M. Gottesdiener, P.J. Larson, K.C. Lasseter, N.G. Agrawal, Absorption, metabolism, and excretion of etoricoxib, a potent and selective cyclooxygenase-2 inhibitor, in healthy male volunteers, Drug Metab. Dispos. 31 (2) (2003) 224–232.
[13] S.H. Lee, R. Bajracharya, J.Y. Min, J.W. Han, B.J. Park, H.K. Han, Strategic approaches for colon targeted drug delivery: an overview of recent advancements, Pharmaceutics 12 (1) (2020) 68.
[14] A. Akhgari, Z. Heshmati, B.S. Makhmalzadeh, Indomethacin electrospun nanofibers for colonic drug delivery: preparation and characterization, Advanced Pharmaceutical Bulletin 3 (1) (2013) 85.
[15] A. Akhgari, Z. Heshmati, H.A. Garekani, F. Sadeghi, A. Sabbagh, B. S. Makhmalzadeh, A. Nokhodchi, Indomethacin electrospun nanofibers for colonic drug delivery: in vitro dissolution studies, Colloids Surf. B Biointerfaces 152 (2017) 29–35.
[16] Y. Ding, C. Dou, S. Chang, Z. Xie, D.G. Yu, Y. Liu, J. Shao, Core–shell eudragit s100 nanofibers prepared via triaxial electrospinning to provide a colon-targeted extended drug release, Polymers 12 (9) (2020) 2034.
[17] X. Wang, D.G. Yu, X.Y. Li, S.A. Bligh, G.R. Williams, Electrospun medicated shellac nanofibers for colon-targeted drug delivery, Int. J. Pharm. 490 (1–2) (2015) 384–390.
[18] Y. Wang, L. Tian, T. Zhu, J. Mei, Z. Chen, D.G. Yu, Electrospun aspirin/Eudragit/lipid hybrid nanofibers for colon-targeted delivery using an energy-saving process, Chem. Res. Chin. Univ. 37 (3) (2021) 443–449.
[19] Y. Turanlı, F. Acartürk, Fabrication and characterization of budesonide loaded colon-specific nanofiber drug delivery systems using anionic and cationic polymethacrylate polymers, Journal of Drug Delivery Science and Technology 63 (2021), 102511.
[20] A. Oliveira, A. Araújo, L.C. Rodrigues, C.S. Silva, R.L. Reis, N.M. Neves, P. Leão, A. Martins, Metronidazole delivery Nanosystem able to reduce the pathogenicity of Bacteria in colorectal infection, Biomacromolecules 23 (6) (2022) 2415–2427.
[21] M.M. Tomadakis, T.J. Robertson, Pore size distribution, survival probability, and relaxation time in random and ordered arrays of fibers, J. Chem. Phys. 119 (3) (2003) 1741–1749.
[22] C.T. Lim, E.P.S. Tan, S.Y. Ng, Effects of crystalline morphology on the tensile properties of electrospun polymer nanofibers, Appl. Phys. Lett. 92 (14) (2008), 141908.
[23] F. Vasconcelos, A.C. Lima, W. Bonani, C.S. Silva, R.L. Reis, A. Motta, C. Migliaresi, A. Martins, N.M. Neves, Microfluidic-assisted electrospinning, an alternative to coaxial, as a controlled dual drug release system to treat inflammatory arthritic diseases, Biomaterials Advances 134 (2022), 112585.
[24] A. Akhgari, M. Hossein Rotubati, Preparation and evaluation of electrospun nanofibers containing pectin and time-dependent polymers aimed for colonic drug delivery of celecoxib, Nanomedicine Journal 3 (1) (2016) 43–48.
[25] P. Liu, L. Gu, L. Ren, J. Chen, T. Li, X. Wang, J. Yang, C. Chen, L. Sun, Intra-articular injection of etoricoxib-loaded PLGA-PEG-PLGA triblock copolymeric nanoparticles attenuates osteoarthritis progression, Am. J. Transl. Res. 11 (11) (2019) 6775.
[26] P. Arunkumar, S. Indulekha, S. Vijayalakshmi, R. Srivastava, Synthesis, characterizations, in vitro and in vivo evaluation of Etoricoxib-loaded poly (Caprolactone) microparticles–a potential intra-articular drug delivery system for the treatment of osteoarthritis, J. Biomater. Sci. Polym. Ed. 27 (4) (2016) 303–316.
[27] P. Arunkumar, S. Indulekha, S. Vijayalakshmi, R. Srivastava, Poly (caprolactone) microparticles and chitosan thermogels based injectable formulation of etoricoxib for the potential treatment of osteoarthritis, Mater. Sci. Eng. C 61 (2016) 534–544.
[28] S.F. Chou, D. Carson, K.A. Woodrow, Current strategies for sustaining drug release from electrospun nanofibers, J. Control. Release 220 (2015) 584–591.
[29] R. Goyal, L.K. Macri, H.M. Kaplan, J. Kohn, Nanoparticles and nanofibers for topical drug delivery, J. Control. Release 240 (2016) 77–92.
[30] T. Riaz, N. Khenoussi, D.M. Rata, L.I. Atanase, D.C. Adolphe, C. Delaite, Blend electrospinning of poly (Ɛ-Caprolactone) and poly (ethylene Glycol-400) nanofibers loaded with ibuprofen as a potential drug delivery system for wound dressings, Autex Res. J. 23 (1) (2021) 66–76.
[31] A. Martins, A.R.C. Duarte, S. Faria, A.P. Marques, R.L. Reis, N.M. Neves, Osteogenic induction of hBMSCs by electrospun scaffolds with dexamethasone release functionality, Biomaterials 31 (22) (2010) 5875–5885.
[32] B. Chauhan, S. Shimpi, A. Paradkar, Preparation and characterization of etoricoxib solid dispersions using lipid carriers by spray drying technique, AAPS PharmSciTech 6 (3) (2005) E405–E409.
[33] P. Patra, V.S. Seesala, S.R. Soni, R.K. Roy, S. Dhara, A. Ghosh, N. Patra, S. Pal, Biopolymeric pH-responsive fluorescent gel for in-vitro and in-vivo colon specific delivery of metronidazole and ciprofloxacin, Eur. Polym. J. 114 (2019) 255–264.
[34] Y.H. Ho, M.A.T. Ashour, Techniques for colorectal anastomosis, World J Gastroenterol: WJG 16 (13) (2010) 1610.
[35] D.Y. Jeong, S. Kim, M.J. Son, C.Y. Son, J.Y. Kim, A. Kronbichler, K.H. Lee, J.I. Shin, Induction and maintenance treatment of inflammatory bowel disease: a comprehensive review, Autoimmun. Rev. 18 (5) (2019) 439–454.
[36] X. Han, S. Ding, H. Jiang, G. Liu, Roles of macrophages in the development and treatment of gut inflammation, Frontiers in Cell and Developmental Biology 9 (2021), 625423.
[37] J.L. Yip, G.K. Balasuriya, S.J. Spencer, E.L. Hill-Yardin, The role of intestinal macrophages in gastrointestinal homeostasis: heterogeneity and implications in disease, Cell. Mol. Gastroenterol. Hepatol. 12 (5) (2021) 1701–1718.
[38] Y.R. Na, M. Stakenborg, S.H. Seok, G. Matteoli, Macrophages in intestinal inflammation and resolution: a potential therapeutic target in IBD, Nat. Rev. Gastroenterol. Hepatol. 16 (9) (2019) 531–543.
[39] S. Guo, R. Al-Sadi, H.M. Said, T.Y. Ma, Lipopolysaccharide causes an increase in intestinal tight junction permeability in vitro and in vivo by inducing enterocyte membrane expression and localization of TLR-4 and CD14, Am. J. Pathol. 182 (2) (2013) 375–387.
[40] D. Wang, R.N. DuBois, The role of COX-2 in intestinal inflammation and colorectal cancer, Oncogene 29 (6) (2010) 781–788.
[41] S.J. Desai, B. Prickril, A. Rasooly, Mechanisms of phytonutrient modulation of cyclooxygenase-2 (COX-2) and inflammation related to cancer, Nutr. Cancer 70 (3) (2018) 350–375.
[42] B. Ruder, R. Atreya, C. Becker, Tumour necrosis factor alpha in intestinal homeostasis and gut related diseases, Int. J. Mol. Sci. 20 (8) (2019) 1887.